Chem Soc Rev

Dynamic Article Links

Cite this: *Chem. Soc. Rev.*, 2011, **40**, 3391–3404

www.rsc.org/csr

**TUTORIAL REVIEW**

# Beating cancer in multiple ways using nanogold†

**Erik C. Dreaden, Megan A. Mackey, Xiaohua Huang,‡ Bin Kang§ and Mostafa A. El-Sayed***

***Received 12th November 2010***
**DOI: 10.1039/c0cs00180e**

Gold nanoparticles possess a unique combination of properties which allow them to act as highly multifunctional anti-cancer agents (X. H. Huang, P. K. Jain, I. H. El-Sayed and M. A. El-Sayed, *Nanomedicine*, 2007, **2**, 681–693; P. Ghosh, G. Han, M. De, C. K. Kim and V. M. Rotello, *Adv. Drug Delivery Rev.*, 2008, **60**, 1307–1315; S. Lal, S. E. Clare and N. J. Halas, *Acc. Chem. Res.*, 2008, **41**, 1842–1851; D. A. Giljohann, D. S. Seferos, W. L. Daniel, M. D. Massich, P. C. Patel and C. A. Mirkin, *Angew. Chem., Int. Ed.*, 2010, **49**, 3280–3294). Not only can they be used as targeted contrast agents for photothermal cancer therapy, they can serve as scaffolds for increasingly potent cancer drug delivery, as transfection agents for selective gene therapy, and as intrinsic antineoplastic agents. This *tutorial review* will highlight some of the many forms and recent applications of these gold nanoparticle conjugates by our lab and others, as well as their rational design and physiologic interactions.

## Introduction

Gold nanoparticle conjugates exhibit properties unique from both their parent molecules and their particle scaffolds. They can show increased binding affinity and targeting selectivity when functionalized with multiple targeting groups, as well as tumor-selective uptake due to their size. Gold nanoparticle conjugates can be delivered systemically, eliciting low immunogenic responses and demonstrating long circulatory half lives. Anti-cancer drug transport kinetics can be rapidly increased by endocytosis of nanoparticle conjugates and poorly soluble chemotherapeutic compounds can be effectively delivered by gold nanoparticle functionalization. Gold nanoconjugates can be co-labeled with imaging contrast agents, molecules to direct intracellular localization, or nucleic acid sequences for targeted anti-cancer gene therapy. These nanoparticles also possess unique optical and electronic properties which can be exploited in cancer-selective photothermal therapeutic applications or non-invasive diagnostic imaging. Their intrinsic size, shape, and surface reactivity can further be used to direct and selectively modify cellular processes associated with malignant progression. Gold nanoparticles represent a versatile, potent, selective, and highly multi-functional anti-cancer technology.[1–4] The following section will discuss some strategies for the synthesis/design of biomedical gold nanoparticle conjugates, as well as their applications in photothermal therapy, drug delivery, gene therapy, and cell cycle regulation.

*Laser Dynamics Laboratory, Department of Chemistry and Biochemistry, Georgia Institute of Technology, Atlanta, GA 30332-0400, USA. E-mail: melsayed@gatech.edu; Fax: +1 404 894 4066; Tel: +1 404 894 0292*

† *Abbreviations*: computed tomography (CT), continuous wave (cw), doxorubicin (DOX), enhanced permeability and retention (EPR), estrogen receptor (ER), human epidermal growth factor receptor 2 (HER2), human umbilical vascular endothelial cells (HUVEC), hydrodynamic diameter (HD), immunoglobulin G (IgG), magnetic resonance imaging (MRI), methotrexate (MTX), near-infrared (NIR), photodynamic therapy (PDT), photothermal therapy (PTT), poly(ethylene glycol) (PEG), poly(lysine) (PLL), poly(styrene sulfonate) (PSS), poly(vinylpyrrolidone) (PVP), positron emission tomography (PET), radio frequency (RF), reticuloendothelial system (RES), RNA interference (RNAi), second harmonic generation (SHG), self-assembled monolayer (SAM), small interfering RNA (siRNA), third harmonic generation (THG), transmission electron microscope (TEM), tumor necrosis factor (TNF), vascular endothelial growth factor 165 (VEGF-165), vascular permeability factor (VPF), X-ray photoelectron spectroscopy (XPS).

‡ Current address: Department of Chemistry, The University of Memphis, 411 Smith Chemistry Bldg, Memphis, TN 38152, USA.
§ Current address: College of Material Science and Technology, Nanjing University of Aeronautics and Astronautics, Nanjing 210016, P.R. China.

## Synthesis, design, and fundamental properties of biomedical gold nanoparticles

### Gold nanoparticle synthesis

Our lab often relies on the use of spherical gold nanoparticles in drug delivery and antineoplastic treatment applications and rod-shaped gold nanoparticles (*i.e.* nanorods) in photothermal therapeutic applications. Small, $\geq 10$ nm, gold nanospheres are synthesized from the reduction of aqueous chloroauric acid by citrate. First observed by Faraday[5] in 1857, the synthesis of colloidal gold generally involves the reduction of a metal salt in the presence of a stabilizing agent. Following the advent of the transmission electron microscope (TEM), Turkevich[6] later surveyed a variety of synthetic methods to

obtain gold nanoparticles and in 1973, Frens[7] systematically developed methods for synthesizing gold nanospheres of varying diameter by citrate-mediated reduction. The resulting nanoparticle sizes are largely governed by the stoichiometric ratio of gold to the reducing agent with larger ratios leading to larger diameters. In this case, citrate also acts as a labile, anionic capping agent which stabilizes the colloid by electrostatic repulsion. Gold nanorods (Fig. 1a) are synthesized by the so-called "seed-mediated growth" method. In this method, small (3–5 nm dia) seeds capped by an amphiphilic, cationic surfactant are synthesized from the reduction of aqueous chloroauric acid by borohydride in the presence of the surface stabilizer. An aqueous chloroauric acid growth solution containing silver nitrate and the stabilizer is then mildly reduced from $Au^{3+}$ to $Au^{+}$ by the addition of ascorbic acid. The seeds are then introduced into the growth solution, acting as nucleation sites for the anisotropic reduction of $Au^{+}$ ions onto the seeds, forming rods over the next several hours. Although the widths of the nanorods formed by this method are fairly constant, lengths can be extended by increasing addition of silver nitrate or other aryl ammonium salts. Gold nanorods were first synthesized electrochemically by Martin using oxide film templates and later by Wang using surfactant-directed electrochemical growth. Murphy and El-Sayed further adapted and optimized the surfactant-directed method for solution-phase growth using the seed-mediated method.[8]

Core–shell, or nanoshell, particles (Fig. 1b) were experimentally developed by Halas and co-workers in the late 1990's due to the predicted high sensitivity of the nanoshell's surface plasmon resonance wavelength to its shell thickness.[3,9] In this synthesis, small, anionic gold nanoparticles are electrostatically adsorbed to the surface of amine-modified silica nanoparticles

**Erik C. Dreaden**

*Erik C. Dreaden received his BS Chem from the University of Georgia in 2006 where he worked with John L. Stickney on the electrochemical deposition of compound semiconductor nanofilms. He is currently a PhD candidate in the School of Chemistry and Biochemistry at Georgia Institute of Technology, studying under Mostafa A. El-Sayed. His research interests include the design, synthesis, and preclinical evaluation of anti-cancer gold nanoparticle conjugates. In the past, he has conducted research in experimental and computational plasmonics, as well as ultrafast laser spectroscopy of semiconductor–metal hybrid nanomaterials.*

**Megan A. Mackey**

*Megan A. Mackey received her BA Chem from the State University of New York at New Paltz in 2007. She worked with Pamela St. John on studying physical properties of DNA hairpin structures. She is currently a PhD candidate in the School of Chemistry and Biochemistry at Georgia Institute of Technology studying under Mostafa A. El-Sayed. Her research involves investigating the fundamental interactions between various gold nanostructures and biological systems as well as the application of these nanostructures in the diagnosis and treatment of cancer.*

**Bin Kang**

*Bin Kang received his BS in applied chemistry from Nanjing University of Aeronautics and Astronautics (NUAA) in China. He is currently a PhD student in material science and engineering at NUAA. He has been supported by the China Scholarship Council and worked at Georgia Institute of Technology as a joint PhD student under the guidance of Prof. M. A. El-Sayed during 2008–2010. His research interests focus on the physical interactions of nanomaterials (mainly carbon nanotubes and gold nanoparticles) with live cells and the development of nanosystems for cancer diagnostics and therapeutics.*

**Mostafa A. El-Sayed**

*Mostafa A. El-Sayed obtained his BSc from Ain Shams University in 1953 and his PhD from Florida State University in 1959 with Michael Kasha. He joined the faculty at UCLA in 1961 and Georgia Tech later in 1994. He is an elected member of the US National Academy of Science, an elected fellow of the American Academy of Arts and Sciences, former editor-in-chief of the Journal of Physical Chemistry, and recipient of the US National Medal of Science. His current research interests include the fundamental optical and electronic properties of nanomaterials and their applications in nanocatalysis, nanomedicine, and photobiology.*

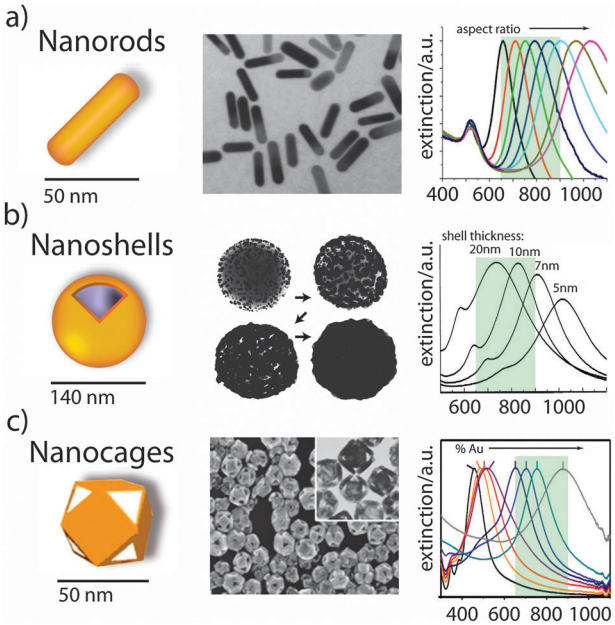


**Fig. 1** Various gold nanostructures commonly used in anti-cancer diagnostic and therapeutic applications. Graphical illustrations, transmission electron micrographs, and synthetically tunable extinction spectra for (a) gold nanorods, (b) gold nanoshells, and (c) gold nanocages. Spectral red-shifts are indicated for increasing aspect ratio, decreasing shell thickness, and increasing gold displacement, respectively. The near infrared (NIR) tissue transmission window is depicted as a green box in each of the spectra. Reprinted with permission from ref. 8, 9, 10, and 11 (panels a, b, c, and c, respectively). Copyright. 2009 Wiley-VCH Verlag GmbH & Co. KGaA, 1998 Elsevier Science B.V., 2006 American Chemical Society, and 2007 Nature Publishing Group/Macmillan Publishers Ltd., respectively.

and used as nucleation sites for the additional chemical reduction of gold, eventually forming a conformal shell around the silica core. Briefly, silica nanoparticles are synthesized by base-catalyzed sol–gel condensation of an orthosilicate (*i.e.* the Stöber method) and surface functionalized with an aminosilane. Small (2–3 nm dia) anionic gold nanoparticles are synthesized by tetrakis(hydroxymethyl)phosphonium chloride (THPC) reduction of aqueous chloroauric acid and electrostatically adsorbed to the surface of the amine-functionalized silica nanoparticle cores. The gold nanoparticle-bound silica cores are then added to a mildly reduced aqueous chloroauric acid solution and formaldehyde is used to reduce additional gold onto the particles, yielding a conformal gold nanoshell. Carbon monoxide was later identified as a preferred reducing agent to formaldehyde, as it forms thinner and more uniform gold nanoshells.

Gold nanocages[10,11] (Fig. 1c) comprise yet another class of biomedically-relevant gold nanostructures. Over the past several years, Xia and co-workers have developed a variety of solution-phase techniques for the synthesis of hollow-core noble metal nanostructures based on the galvanic displacement method. The technique relies on the use of a metal nanoparticle template from which atoms are displaced for another metal. The precursor nanoparticle is comprised of a less noble metal (*e.g.* Ag) such that the addition of ions of a more noble metal (*e.g.* Au, Pt, Pd) will spontaneously replace those on the precursor particle. Gold nanocages are made by reacting silver nanocubes with $Au^{3+}$ ions. Because the reduction potential of gold is more positive (*i.e.* more energetically favorable) than silver, atoms from the silver cube are spontaneously oxidized/displaced as gold ions are reduced onto the precursor particle surface. In this case, because gold reduction is a three electron process and silver oxidation is a one electron process, voids are created in the newly formed cuboid structure as three silver atoms are exchanged for one gold atom. Displacement proceeds according to the availability of surface sites afforded by the particle capping agent's affinity for specific crystallographic facets of the template particle, in the case of silver cubes forming a subsequent cage-like gold structure.

## Conjugation

The gold nanoparticle surface represents one of the most stable and easily functionalized platforms for molecular conjugation. Au surfaces can be functionalized with a variety of organic self-assembled monolayers (SAMs)[12] (*e.g.* thiolates, dithiolates, amines, carboxylates, cyanides, isothiocyanates, phosphines, *etc.*) to allow stable dispersion of particles in both aqueous and organic media. In most cases, ligation is spontaneous at room temperature and occurs over the millisecond to minute time scale for commonly used alkanethiols. Packing and reordering of the SAM can occur over several hours and place exchange of the monolayer can also be performed to functionalize gold nanoparticles with mixed monolayers or fully exchanged SAMs of targeting, therapeutic, or stabilizing ligands, as well as heterobifunctional linkers to which such molecules can also be appended. Gold adsorbate coverages can be as high as $1.5 \times 10^{15}$ molecules $cm^{-2}$, however in practice, coverages are typically an order of magnitude less.[13]

Multivalent nanoparticle conjugates exhibit cellular interactions distinct from their parent ligands or particles. Similar to antibodies, nanoconjugate binding affinity ($K_D$) can be enhanced by simply increasing the density of targeting ligands on the particle, in some cases increasing the affinity up to 4 orders of magnitude.[14] The circulatory half life of hydrophobic drugs can also be significantly increased by functionalization with hydrophilic nanoparticles.[15] The intracellular transport rate of molecules which passively diffuse into the cell can be enhanced by endocytosis of their nanoparticle conjugates,[16] the intracellular localization of drugs can be directed by cell-penetrating peptides or nuclear localization sequences,[17] and endosomal sequestration/degradation can be escaped by proton sponge groups or photothermal heating[18] of the particle. Targeting selectivity and tumor accumulation of the nanoparticle conjugate can be further enhanced using multiple targeting groups and therapeutic response can be greatly increased using multimodal, "cocktail-based" oncologic approaches.

## Biocompatibility

Stability is another important aspect in the design of oncologic gold nanoparticle conjugates. Physiological environments exhibit high ionic and serum concentrations which can disrupt and diminish the stabilizing capacity of many nanoparticle ligands. Nanoparticles are considered stably suspended if the working distance of their repulsive forces outweighs that of

their attractive forces. Attractive forces are generally attributed to van der Waals interactions and repulsive forces are generally associated with charge–charge (*i.e.* electrostatic) or physical (*i.e.* steric) separation. Because of the high ionic concentration present in both physiologic fluids and cell growth media, electrostatic repulsion alone is often insufficient to overcome Debye charge screening and subsequent nanoparticle aggregation. Physical separation using hydrophilic polymer ligands is common practice and allows stable suspension of the particles in both high ionic strength and serum concentration environments. Poly(ethylene glycol) (PEG) is the most common surface ligand used to stabilize biomedical nanoparticles and is particularly amenable to gold surfaces by way of a thiol linker. PEG consists of hydrophilic poly(ethylene oxide) repeats and can be branched if increased stability and size are desirable. Gold nanorods have, for example, exhibited circulatory half lives as high as 17 h in nude mice when PEGylated.[15] Other common polymer stabilizers for gold nanoparticles include: poly(lysine) (PLL), poly(styrene sulfonate) (PSS), starches, and poly(vinylpyrrolidone) (PVP). Functionalization with such polymers not only increases hydrophilicity, but also decreases immunogenic response from the nanoparticles, as well as their recognition/removal by the reticuloendothelial system (RES) by minimizing adsorption of proteins and molecules (*i.e.* opsonins) which initiate phagocytic uptake. Together, these strategies serve to maximize circulatory half life and, thus, tumor accumulation by active or passive targeting strategies.

Aseptic handling procedures should be utilized throughout the synthesis, conjugation, and purification steps to minimize contamination of *in vitro* cultures and potential misinterpretation of experimental results, cytotoxicity, *etc*. Improper handling during *in vivo* experiments can further lead to infection, thrombosis (*i.e.* blood clots), and acute immune responses. Readers should also note that the use of unstabilized and/or uncoated gold nanoparticles, apart from being physiologically unstable, typically results in significant cyto/genotoxicity and is therefore avoided in all current biomedical applications.

## Optical properties

Metallic conductors are characterized by their delocalized electrons (*i.e.* free, or Drude-like electrons) whose density can vary in response to an externally applied electromagnetic field. Just as solid materials exhibit vibrational modes associated with the collective oscillations of their atoms, metallic solids also exhibit collective oscillatory modes of their free electrons—plasmon modes or polaritons. Free electrons in noble metals exhibit plasmon oscillation frequencies in the mid- to far- UV; those at their surfaces, however, are less restricted and can oscillate at near-UV, optical, NIR, and IR wavelengths.

Incident electromagnetic fields (*i.e.* photons) can couple with surface plasmon modes of similar angular momentum and frequency, leading to their absorption or scattering. Surface plasmon resonance—often simply "plasmon resonance"—results in the local increase of resonant electromagnetic fields over several orders of magnitude and is known to enhance a number of radiative and non-radiative processes such as absorption, optical rotation, fluorescence, Raman scattering, Mie scattering, second- and third- harmonic generation (SHG and THG), hyper-Rayleigh scattering, and hyper-Raman scattering. Surface plasmon absorption occurs rapidly, dephasing on the 1–100 femtosecond time scale, dissipating absorbed energy by coupling to adjacent electronic systems (*vide supra*) or to atomic lattice vibrations (*i.e.* phonon modes). Subsequent phonon–phonon relaxation occurs on the picosecond time scale and results in highly localized heat generation.[19] When excited by high fluence pulsed laser sources, intense shock waves (*i.e.* acoustic or water vapor pressure waves) can be generated which are capable of being detected by *ex vivo* ultrasound transducers[20] or, in some instances, disrupting nearby cellular structures.

The wavelength of a nanoparticle's surface plasmon resonance depends on the metal, as well as its size, shape, and dielectric environment. Plasmonic metals include Li, Na, K, Mg, Al, Fe, Cu, Ag, Pt, and Au. Of these, gold is the only nanoscale metal which exhibits both inert reactivity and plasmon resonance which is red shifted sufficient to avoid significant incident field attenuation by tissues and fluids in physiologically relevant environments.

Increased size can serve to red shift gold's surface plasmon resonance from its *ca.* 520 nm spherical particle resonance (in water) as a result of optical retardation of the incident wave as it propagates through the particle and is dephased. Size-dependent shifts are most often insufficient to achieve high tissue penetration wavelengths, however. With increasing size, absorption quantum yields also diminish due to increased scattering, a property which can often be disadvantageous. Although the dielectric environment surrounding circulating and tissue-accumulated nanoparticles is fairly constant, surface plasmon resonance can also red shift significantly with increasing dielectric permittivity and refractive index. In order to shift plasmon resonance to high tissue penetration wavelengths, most researchers synthetically vary the shape of their gold nanoparticles. This can be accomplished by increasing the aspect ratio of a rod-shaped nanoparticle or by decreasing the shell/wall thickness of a core–shell or hollow core nanoparticle.

## Accumulation, uptake, and clearance

One particular advantage of anti-cancer gold nanoparticle conjugates is their size-selective accumulation at tumor sites due to the enhanced permeability and retention (EPR) effect.[21] Malignant cells require larger amounts of nutrients in order to sustain their accelerated growth and division. To meet this demand, solid tumors stimulate the production of new vasculatures through which increasing amounts of blood can be supplied (*i.e.* angiogenesis). In contrast to normal vessels, the angiogenic neovasculature is characterized by a highly disordered endothelium with large gaps that permit the preferential penetration of nanosized conjugates (Fig. 2). Characteristically diminished lymphatic drainage from the tumor interstitium also serves to increase retention of such compounds at the tumor site, resulting in both augmented penetration and decreased clearance of circulating nanoconjugates. The EPR effect has been demonstrated using a

 

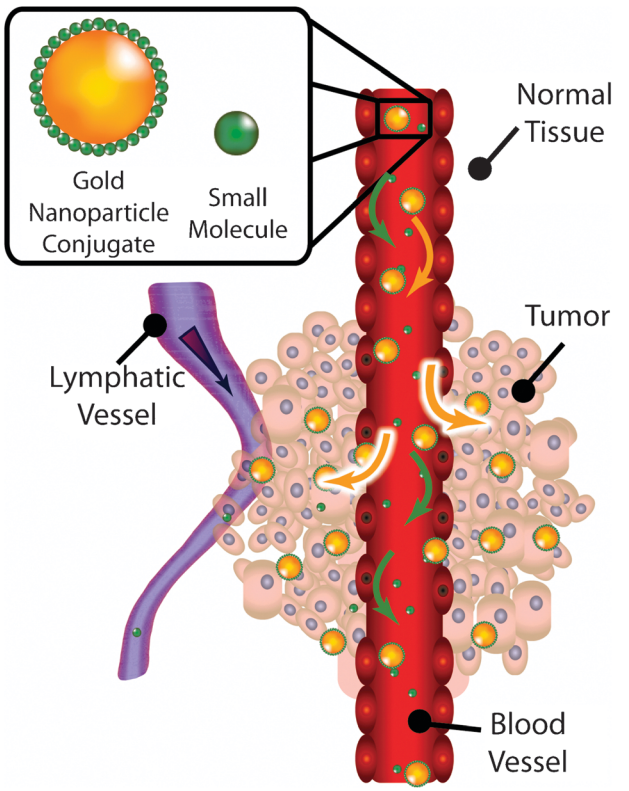


**Fig. 2** Graphic illustrating the size-selective preferential accumulation of circulating gold nanoparticle conjugates at tumor sites by the enhanced permeability and retention (EPR) effect. Large gold nanoparticle conjugates preferentially penetrate through blood vessels at tumor sites due to their disordered endothelial cells while smaller molecules continue to circulate. Diminished lymphatic drainage at the tumor site also serves to reduce the clearance of these gold nanoparticle conjugates from the tumor interstitium.

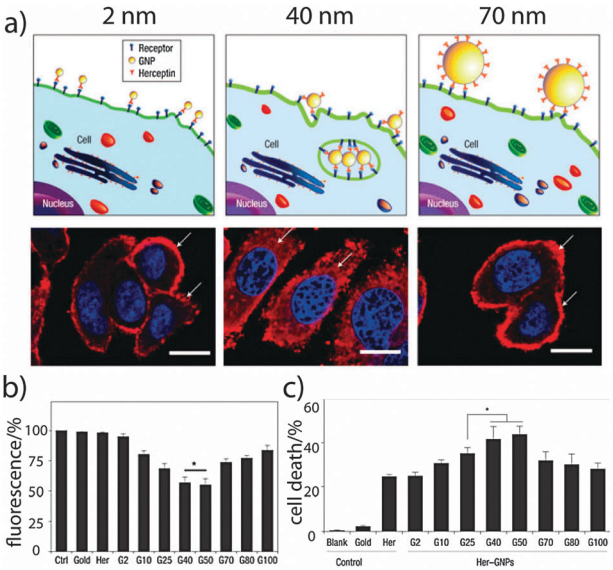


**Fig. 3** Size-dependent receptor-mediated endocytosis of antibody-gold nanoparticle conjugates. Schematic (a) illustrating how nanoconjugate size and receptor density affect EGFR-mediated uptake of Herceptin-labeled gold nanoparticles into SK-BR-3 breast cancer cells. 2 nm gold nanoparticles were not efficiently internalized because multiple receptors could not be simultaneously bound. 70 nm particles exhibited multivalent binding, however they were too large for efficient membrane wrapping (*i.e.* endocytosis). Increased relative fluorescence intensity (b) associated with nanoparticle uptake was found to correlate well with subsequent therapeutic response (c). Nuclei are stained blue, scale bar = 10 μm, $*p < 0.05$, error bars ±sd, $n = 4$. Reprinted with permission from ref. 26. Copyright 2008 Nature Publishing Group/ Macmillan Publishers Ltd.

variety of protein/DNA/polymer complexes, as well as nanoparticles including micelles, liposomes, metal nanostructures, and quantum dots. As one would expect, the optimal size for EPR of a gold nanoparticle conjugate varies depending on the stage, location, and type of cancer, however particles with a hydrodynamic diameter (HD) greater than the renal clearance threshold (*ca.* 6 nm) and up to 2 μm in HD can be expected to exhibit preferential tumor accumulation. Passively[22,23] (*e.g.* EPR) and actively[22–24] targeted gold nanoparticles, for example, have exhibited as much as 2–5% and 6–13% tumor accumulation, respectively, from systemically administered particles *in vivo*.

Although most gold nanoparticle conjugates are capable of exhibiting some degree of intracellular penetration, particle size, charge, and lipophilicity also play critical roles in determining the extent of uptake. Chan and co-workers have studied the size- and shape-dependent intake of gold nanoparticles by cervical cancer cells (HeLa) and found that size-dependent internalization peaked at a 50 nm diameter (bare) and that the uptake of colloidal nanorods decreased with increasing aspect ratio.[25] In another study using immunoglobulin G (IgG) antibody gold nanoparticle conjugates, they further found that multivalent functionalization of smaller gold nanoparticles did not enhance uptake due to their decreased ability to occupy multiple, receptor binding sites and that larger particles, although capable of multivalent receptor binding, were too large for membrane wrapping (*i.e.* engulfing) necessary for efficient endocytosis (Fig. 3).[26] Here, particles conjugated to antibodies of an epidermal growth factor receptor (EGFR) exhibited greatest uptake into breast cancer cells (SK-BR-3) and therapeutic response when 40–50 nm (bare dia) gold nanoparticles were used. Although the optimal particle size for intracellular penetration obviously varies depending on the cell size, type, receptor density, metabolic activity, *etc.*, as well as the specific targeting strategy employed (*i.e.* IgG, fragments thereof, *etc.*), this study nonetheless highlights the importance of therapeutic nanoconjugate size in determining subsequent transport kinetics and treatment efficacy. Cationic zeta potential (*i.e.* positive surface charge) can also promote the uptake of nanoconjugates due to electrostatic attraction with anionic cell-surface proteoglycans. In some cases however, this attraction can result in significant cytotoxicity due to membrane disruption. Lipophilicity, as measured by the octanol:water partition coefficient (log *P*) further promotes nanoparticle-cellular interaction and uptake by association with hydrophobic cell-surface and extracellular matrix domains. Due to poor aqueous stability and low circulatory half life however, highly lipophilic gold nanoparticles are typically co-conjugated with hydrophilic polymer stabilizers such as PEG.

The pharmacokinetic clearance of circulating gold nanoparticle conjugates is also of key importance to subsequent efficacy.[27] Polyanionic gold nanoparticles up to 4–6 nm in HD typically exhibit efficient urinary (renal) excretion while polycationic particles up to 6–8 nm in HD can be similarly cleared. The increased propensity for polycationic urinary excretion is due to electrostatic attraction with the net negative charge of the capillaries which separate circulating blood from urinary filtrates. Although efficient urinary clearance is sometimes desirable, polycationic nanoparticles can exhibit poor circulatory half lives due to electrostatic attraction with the negatively charged laminar surfaces of the blood vessels. Polyanionic nanoparticles, on the other hand, often exhibit decreased cell penetration. Nanoparticle opsonization and phagocytic uptake are typically lowest when particles are neutral in zeta potential and contain hydrophilic polymers which shield hydrophobic–hydrophobic and/or electrostatic interactions with IgG and serum proteins.[28] In contrast to orally administered drugs which optimally exhibit high lipophilicity (*c* log $P \approx 3$–5), optimal lipophilicity of a therapeutic nanoparticle conjugate can be expected to lie over a range similar to intravenously administered drugs (median *c* log $P \approx 1.92$).[29] Circulating nanoparticles which cannot be filtered by the renal system (*i.e.* kidneys) are captured and degraded by Kupffer cells or allowed to proceed to the liver where they are metabolized by (or accumulated in) hepatocytes and excreted into the bile.

Cho *et al.* have recently studied the size-dependent *in vivo* accumulation and clearance of intravenously administered, thiol-PEGylated (5 kDa) gold nanoparticles in nude mice.[30] They found that larger gold nanoparticles (100 nm *versus* 4 and 13 nm dia) exhibited shorter circulatory half lives and more rapid RES accumulation. Smaller gold nanoparticles (4 and 13 nm dia) accumulated predominantly in the liver, spleen, and lung, reaching peak accumulation at 7 days and persisting up to 6 months. In contrast, larger 100 nm dia particles accumulated predominantly in the liver and spleen, rapidly reaching maximum accumulation at 30 min and also persisting for the 6 month duration of the study. Very low urinary excretion of the small gold nanoparticles was shown over 1 day post-injection and only nominal renal clearance of the large particles was observed. Very low biliary excretion was also shown for all particles up to 1–4 weeks, however the majority of the particles remained accumulated in the RES organs. While little acute and subacute toxicity has been observed from *in vivo* administration of polymer-stabilized therapeutic gold nanoparticle conjugates, further long term toxicological investigations are clearly needed in order to accelerate clinical translation of these technologies, particularly with respect to maintenance of RES organ function, effects from potential chronic inflammation, potential mutagenicity, and effects on reproductive health. Viable strategies to facilitate hepatobiliary clearance of these drugs is also urgently needed.

## Applications of anti-cancer gold nanoparticle conjugates

### Gold nanoparticles as photothermal contrast agents

Photothermal therapy (PTT) is a cancer treatment method which, like chemotherapy, relies on the selective application or the increasing sensitivity of cancer cells to cytotoxic damage—in this case from heat, or hyperthermia. A wide variety of electromagnetic radiation sources can be used in these treatments, applied in whole-body procedures or focused to specific regions of interest, where it is absorbed and dissipated as heat by intrinsic (*i.e.* physiologically endogenous) molecules such as melanin and water, or by photothermal contrast agents which can be directly applied to solid tumors or intravenously administered and accumulated at malignant sites by active/passive targeting. Although the methodology has gained some degree of popularity in Europe, it is not yet widely applied in clinical settings in the US. Current clinical and preclinical PTT trials using gold nanoparticle contrast agents, however, are rapidly progressing (*e.g.* CytImmune, Nanospectra Biosciences).

Photothermal therapies involving plasmonic gold nanoparticles can be categorized based on the mechanisms by which they achieve cell death. Mild temperature increases (*i.e.* hyperthermia, 3–6 °C) often proceed *via* apoptotic pathways and are well known to perturb a variety of normal cellular functions. These can result in denaturation of proteins/enzymes, induction of heat-shock proteins, metabolic signaling disruption, endothelial swelling, microthrombosis, diminished vascular supply, impaired receptor recognition, dysfunctional membrane transport, and inhibited nucleotide synthesis.[31,32] Further, the ability of malignant cells to repair such damages is also decreased (*versus* normal cells). Because of its mild impact and minimal side effects, hyperthermic treatments are typically prolonged/recurrent and effects can often be dramatic—the so-called "Lance Armstrong Effect".[33] Larger, more rapid temperature increases, often termed "ablative" treatments, occur by necrotic cell death. In these cases, disruption of the cellular membrane is often predominant, however cavitation and subsequent physical destruction of organelles can also occur.

Gold nanoparticles are currently being explored as contrast agents for anti-cancer PTT because their absorption cross sections and photostabilities are far superior to traditional molecules such as indocyanine green. Treatments can include focused and fiber optic-guided laser excitation of primary tumors, and can be particularly advantageous in treating tumors in areas poorly accessible by surgery or with ill-defined margins. Because absorption by physiological fluids and tissues (*e.g.* oxy/deoxyhemoglobin and water) is minimal in the near-infrared (*i.e.* 650–900 nm) region, the absorption maxima of therapeutic and diagnostic gold nanoparticles are synthetically tuned to this "NIR window" (Fig. 4).[34] Microwatt NIR lasers (FDA class 1) can, for example, efficiently penetrate as much as 4 cm through skull/brain and deep muscle tissue and 10 cm through breast tissue. Higher power lasers (FDA class 3) have exhibited 7 cm penetration depths through muscle and neonatal skull/brain tissue, as well. In PTT applications, gold nanorod, nanoshell, and nanocage absorption is tuned by synthetically varying the aspect ratio, shell thickness : core radius, and the extent of galvanic displacement, respectively (Fig. 1).

PTT using gold nanoparticles was first demonstrated *in vitro* by Lin and co-workers in 2003.[35] Here, spherical gold nanoparticles were conjugated to IgG antibodies which targeted

 

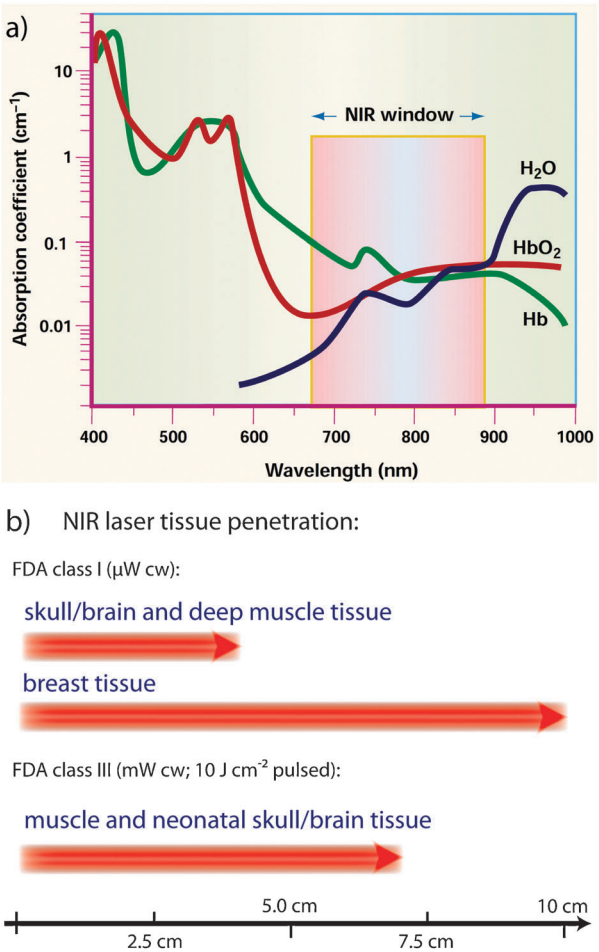


**Fig. 4** Wavelength range of the near-infrared (NIR) tissue transmission window. In the 650–900 nm spectral range (a), absorption from physiologic fluids such as oxy/deoxyhemoglobin and water is minimal, allowing maximum penetration depths (b) for external laser radiation. Photothermal therapy, photoacoustic tomography, and optical diagnostic imaging are most efficient in this range. Gold nanoparticle contrast agents are designed to optimally absorb in these regions. Reprinted with permission from ref. 34. Copyright 2001 Nature Publishing Group/Macmillan Publishers Ltd.

CD8 receptors on peripheral blood lymphocyte cells. Using nanosecond pulsed visible laser exposure, 95% of cells containing as few as *ca.* 500 particles cell$^{-1}$ were killed (*versus* 5–8% in sham treatments) due to apparent membrane disruption. Our lab later demonstrated the use of continuous wave visible laser exposure in PTT of oral squamous cell carcinoma cells treated with spherical gold nanoparticle conjugates of EGFR IgG antibodies.[36] Benign cells were found to require more than twice the energies required to kill malignant cells due to increased antibody–nanoparticle conjugate labeling and PTT response from the cancer cells.

Halas and West later applied silica–gold core–shell nanoparticles in near-infrared PTT, correlating *in vitro* treatment response with *in vivo* efficacy.[37] Breast carcinoma cells specifically labeled with PEGylated gold nanoshells were shown to be efficiently destroyed by cw NIR laser exposure (7 min, 35 W cm$^{-2}$, 5 mm spot dia). The nanoshells were later

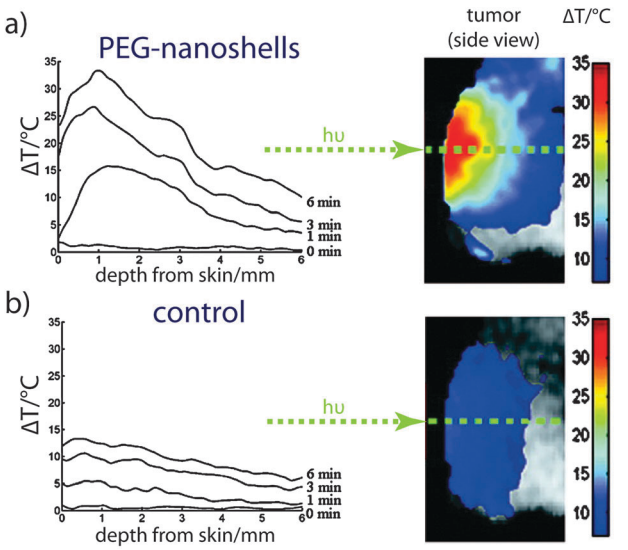


**Fig. 5** Real-time, *in vivo* magnetic resonance imaging (MRI) guidance and temperature monitoring of near-infrared (NIR) laser photothermal cancer therapy using locally administered gold nanoshells. PEGylated silica–gold core–shell nanoparticles were injected into the tumor interstitium of *scid* mice bearing sarcoma xenografts. MRI was used to guide NIR laser exposure and to three dimensionally map subsequent temperature increases for (a) nanoshell-treated and (b) sham-treated tumors based on the temperature-dependent MRI frequency shift of protons in the tissues. Reprinted with permission from ref. 37. Copyright 2003 National Academy of Sciences, USA.

injected into the tumor interstitium of *scid* mice bearing sarcoma xenografts. Using magnetic resonance imaging (MRI), NIR laser exposure was directed about the tumor site (4 W cm$^{-2}$, 5 mm spot dia, $<$6 min). Based on the temperature-dependent MRI frequency shift of protons in the tissues, intratumoral temperature changes were three dimensionally mapped in real time (Fig. 5), showing average temperature increases of 37.4 $\pm$ 6.6 °C in nanoshell treated PTT (*versus* 9.1 $\pm$ 4.7 °C in sham PTT) which histological analysis found resulted in significant coagulation, cell shrinkage, and loss of nuclear staining. NIR PTT using systemically administered nanoshells was later demonstrated using a colon cancer model.[38] PEGylated gold nanoshells were intravenously injected in carcinoma-bearing nude mice and their tumors were exposed to cw NIR laser radiation after 6 h accumulation (4 W cm$^{-2}$, 3 min, 5.5 mm spot dia). Tumors in nanoshell treated mice were completely ablated after a single PTT treatment and the animals appeared healthy and tumor free $>$90 days post treatment. In contrast, tumors in control and sham-treated animal groups continued to grow, with nearly 50% mortality at day 10.

El-Sayed and co-workers later demonstrated *in vitro* NIR PTT using gold nanorods which can more efficiently absorb photons to generate heat.[39] Anti-EGFR conjugates of gold nanorods were found by dark-field scattering microscopy to selectively label oral squamous cell carcinoma cells which overexpress cell-surface EGFR. Similar to experiments with gold nanospheres, cw laser NIR PTT found that malignant cells required nearly half the energy necessary to kill non-malignant cells due to their increased labeling and associated

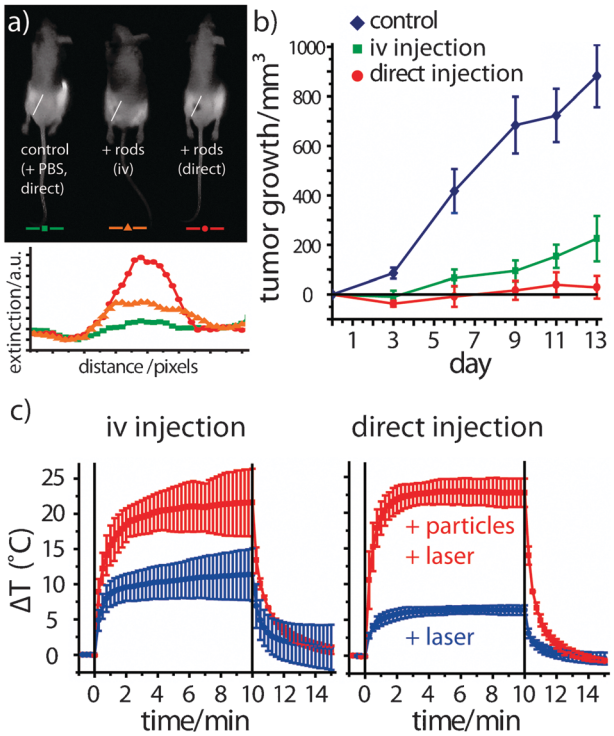


**Fig. 6** *In vivo* near-infrared (NIR) laser photothermal therapy using gold nanorod contrast agents. PEGylated gold nanorods were intravenously and locally injected in carcinoma-bearing nude mice. NIR imaging (a) indicated significantly increased NIR laser absorption/scattering by nanorods accumulated at the rear flank tumor sites. Changes in tumor volume (b) were recorded over two weeks following a single laser exposure, indicating significant tumor growth remission for both direct and intravenous nanorod administration, as well as resorption of >57% of the directly-injected tumors and 25% of the intravenously-treated tumors. Real-time, intratumoral temperature probe measurements (c) correlated enhanced (>20 °C) heating of nanorod-treated tumors with tumor resorption/remission. Reprinted with permission from ref. 32. Copyright 2008 Elsevier Science B.V.

membrane disruption from the treatments. The group later demonstrated the use of both systemically and locally administered gold nanorods in *in vivo* NIR PTT (Fig. 6).[32] PEGylated gold nanorods were intravenously or interstitially administered in nude mice bearing squamous cell carcinoma tumors. The gold nanorods exhibited efficient accumulation and enhanced NIR absorption at the tumor site following administration by both methods. After a single cw NIR laser exposure, nanorod treated tumors exhibited dramatic growth remission (1–2 W $cm^{-2}$, 10 min, 6 mm spot dia). Greater than 57% of the directly-injected tumors and 25% of the intravenously-treated tumors were completely resorbed at day 13. Bahatia and co-workers later showed that the intrinsic X-ray absorbing properties of gold nanorods (which are doubly greater than that of clinical iodine standards) can be used to guide NIR PTT and increase the treatment efficacy.[15] Using X-ray computed tomography (CT) and contrast from tumor-accumulated gold nanorods, they were able to non-invasively image and three-dimensionally reconstruct tumor xenograft margins in nude mice models. Subsequent NIR PTT achieved complete tumor resorption and 100% survival of the nanoparticle treated group, while tumors in sham-treated and control groups grew uncontrolled with ≤1 month survival (0.75 W $cm^{-2}$, 1 min, 1 cm spot dia).

In 2007, Xia and co-workers first demonstrated the use of gold nanocages for contrast in *in vitro* NIR PTT.[40] Nanocages conjugated to antibodies of the human epidermal growth factor receptor 2 (HER2) were used to selectively target breast cancer cells overexpressing cell surface HER2. Cell destruction using pulsed NIR laser exposure was observed at a minimum power density of 1.5 W $cm^{-2}$ (5 min, 2 mm spot dia). Using similarly synthesized hollow-core, spherical gold nanoparticles, Li and co-workers have studied *in vitro* NIR PTT using anti-EGFR conjugates of the hollow gold nanoparticles, as well as their *in vivo* biodistribution following intravenous administration.[24] EGFR overexpressing squamous cell carcinoma cells were found to be selectively labeled and photothermally destroyed using cw NIR laser exposure (40 W $cm^{-2}$, 5 min, 2 mm spot dia). Intravenous administration in tumor bearing nude mice resulted in predominant RES organ (*i.e.* liver, spleen, and kidney) accumulation. Tumor accumulation was found to be as high as 6.5% of the initial dose with predominant perivascular localization. Targeted NIR PTT of melanoma tumors using hollow gold nanoparticles was further studied in animal models by the same group using an agonist ligand of a melanocortin type-1 receptor, overexpressed by melanoma cells.[22] Biodistribution studies following 24 h of intravenous circulation found significantly enhanced tumor accumulation by the active targeting strategy (13% *versus* 5%). Histological analysis following NIR laser exposure determined significantly enhanced necrotic response from nanoparticle treated tumors (66% *versus* 8% sham, 0.5 W $cm^{-2}$, 1 min, 1 cm spot dia). Positron emission tomographic (PET) imaging also indicated dramatically decreased (89%) metabolic activity in nanoparticle treated tissues, but not in sham or control tumors. Xia and Wang have further demonstrated that the NIR absorption properties of nanocages and other plasmonic gold nanoparticles can be used to non-invasively image tumors for surgical or PTT guidance, as well as to assess the stage and location of primary melanoma tumors *in vivo* by photoacoustic tomographic imaging (Fig. 7).[41] Also using a ligand of the melanocortin type-1 receptor, they showed that systemically administered nanocages can be preferentially targeted to melanoma tumors, allowing *ca.* 40% increased imaging contrast and actively-targeted tumor accumulation.

Determining the optimal gold nanostructure for NIR PTT can be highly subjective due to the numerous ways in which such analyses can be performed. Structures can be compared based on their absorption cross sections, absorption efficiencies, or thermal transduction efficiencies on a per particle, per unit gold, per unit mass, or per unit extinction basis. Gold nanorods have been shown to exhibit much larger and narrower NIR absorption cross sections and efficiencies than either nanoshells or nanocages.[42,43] Experiments comparing NIR thermal transduction from solutions of equivalent optical density (*i.e.* extinction) found gold nanorods and $AuS_2$–Au nanoshells to be much more efficient photothermal contrast agents than $SiO_2$–Au nanoshells.[43] Per unit mass gold, nanorods have exhibited 1/3 the spectral bandwidth, *ca.* 3-fold

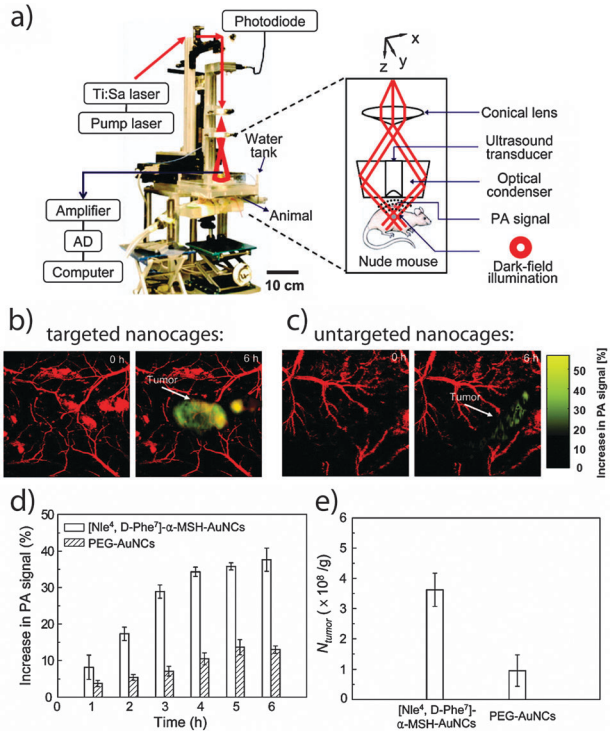


**Fig. 7** Non-invasive, *in vivo* photoacoustic tomographic imaging of melanoma tumors using gold nanocage contrast agents. Laser scanning confocal photoacoustic microscopy (a) of nude mice bearing subcutaneous B16 melanoma tumors was obtained using an ultrasonic transducer and dark-field optical condenser. Blood vessels were imaged at 570 nm and tumors were imaged at the 778 nm peak extinction maxima of the gold nanocages. Percent increase in photoacoustic imaging intensity following intravenous injection of targeted and untargeted (b) nanocages over 6 h indicates *ca.* 40% increased signal (c) from particles targeted to α-melanocyte stimulating hormone (MSH) receptors on the tumors and *ca.* 15% increased signal from passively targeted PEGylated nanocages. Mass spectrometry of nanocage accumulation in the tumors (d–e) correlates increasing photoacoustic signal amplitude with particle accumulation. Reprinted with permission from ref. 41. Copyright 2010 American Chemical Society.

higher extinction cross section, and 6 times greater heating capability than $SiO_2$–Au nanoshells in NIR laser photothermal experiments.[15]

While the scope of this tutorial review is limited to photothermal, drug delivery, and biophysical antineoplastic applications, the audience should also be aware of significant progress in the development of methods for the use of spherical gold nanoparticles as sensitizing agents for radio frequency (RF) ablation and X-ray radiation cancer therapies. Readers are directed to the works of Curley *et al.*[44] (RF), Geller *et al.*[45] (RF), Hainfeld *et al.*[46] (X-ray), and references therein for a comprehensive review of the field.

### Gold nanoparticles as drug delivery scaffolds

In addition to their photothermal and photoacoustic properties, gold nanoparticles are also attractive platforms for the delivery of increasingly potent, selective, and multifunctional anti-cancer drug conjugates. Spherical gold nanoparticles bound to tumor necrosis factor α (TNF) comprise one of the best studied oncologic gold nanoparticle conjugates. TNF is a cytokine protein shown to promote anti-tumor immunogenic response, malignant vascular leakage, and apoptosis in a variety of cancer cell lines. Soluble and membrane-bound TNF receptors can also serve to actively direct the accumulation of TNF at tumor sites. Paciotti and Tamarkin have combined the EPR accumulation of PEGylated gold nanospheres (26 nm dia) with the active targeting and antineoplastic properties of TNF to selectively deliver and treat solid tumors using intravenously administered gold nanoparticle–TNF conjugates.[47] They were able to show 7–10 fold greater TNF tumor accumulation in animal models administered with the nanoparticle conjugate *versus* an equivalent mass of the protein. The TNF–gold nanoparticle conjugates were further demonstrated to be twice as effective as the native molecule in causing tumor regression, achieving complete response in 25–30% of treated animals following a single 7.5 μg dose. The conjugates also showed significantly reduced toxicity relative to equivalent masses of native TNF (0% *versus* 15% mortality). Phase II clinical trials using this technology are currently pending.

In addition to cytokine receptors, hormone receptors can also be used for the selective targeting and delivery of therapeutic gold nanoparticle conjugates. Breast cancer treatment is an excellent candidate for such methods as 75–80% of all breast malignancies overexpress hormone receptors. Our group has recently explored the use of the estrogen receptor (ER) antagonist, tamoxifen, to selectively target and deliver gold nanoparticles to ER+ breast cancer cells with greatly enhanced cytotoxicity (per drug molecule, Fig. 8).[16] Dreaden *et al.* synthesized a thiol-PEGylated tamoxifen derivative which maintained chemotherapeutic efficacy, and could also be easily functionalized onto gold nanoparticle surfaces. The PEG spacer afforded increased *in vitro* stability and would also decrease RES uptake and immunogenic response *in vivo*. Dark-field scattering microscopy indicated ER-selective intracellular particle delivery and dose–response kinetics showed greatly increased rates of tamoxifen influx from the gold nanoparticle conjugate. Potency (per drug molecule) was increased up to 270% due to ER-dependent particle uptake and increasingly rapid drug transport by particle endocytosis rather than passive diffusion of the free drug.

Mirkin and Lippard have also exploited the rapid intracellular uptake of gold nanoparticles to deliver and activate a prodrug form of the widely administered chemotherapeutic, cisplatin (Fig. 9).[48] By conjugating spherical gold nanoparticles (13 nm dia) with an inert $Pt^{4+}$ analog of the cytotoxic drug, cisplatin ($Pt^{2+}$), the group was able to achieve efficient cytosolic delivery of the prodrug to bone, lung, cervical, and prostate cancer cells without endosomal sequestration. Subsequent intracellular reduction of the prodrug caused activation to the cytotoxic $Pt^{2+}$ form, resulting in colocalization of the particles with microtubules and the formation of intrastrand crosslinked nuclear DNA. *In vitro* cytotoxicity was dramatically enhanced over that of the free prodrug and the active cisplatin form, demonstrating gold nanoparticles as efficient vehicles for the delivery of prodrugs exhibiting poor cellular uptake. Similarly enhanced potency has also been demonstrated from gold nanoparticle conjugates of oxyplatin.[49]

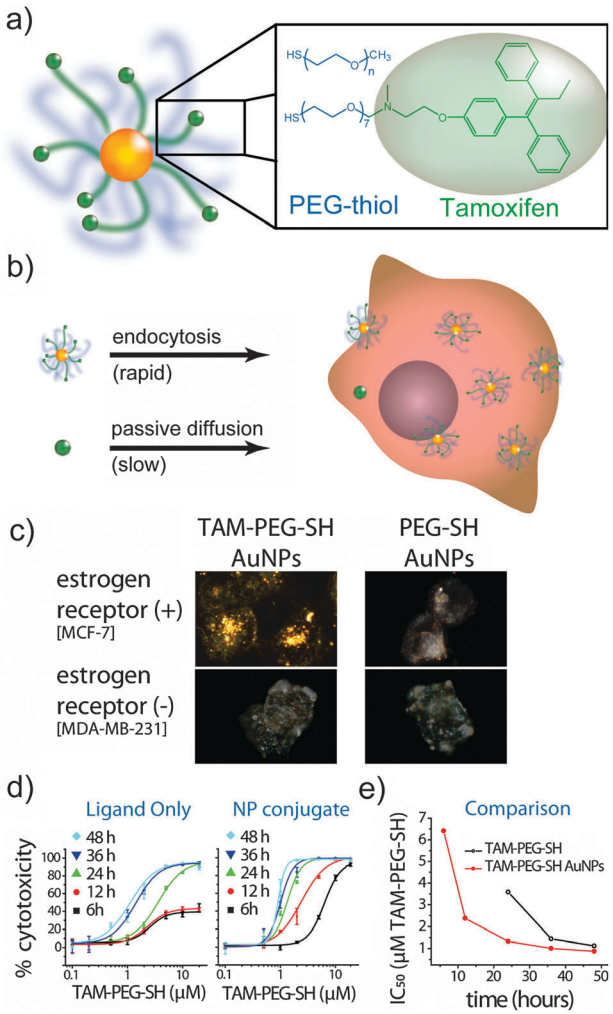


**Fig. 8** Selective delivery and enhanced potency of breast cancer chemotherapeutics by gold nanoparticle conjugation. A derivative of the estrogen receptor antagonist, tamoxifen, was conjugated to gold nanoparticles (a), allowing increasingly rapid and efficacious delivery (b) to breast cancer cells expressing an estrogen receptor. Dark-field scattering microscopy (c) expressing estrogen receptor-selective intracellular particle delivery. Dose–response kinetics (d), estrogen competition, and endocytotic suppression indicated increased rates of drug transport by endocytosis of the nanoparticle conjugate *versus* passive diffusion of the free drug, resulting in up to 2.7 fold enhanced potency per drug molecule. Reprinted with permission from ref. 16. Copyright 2009 American Chemical Society.

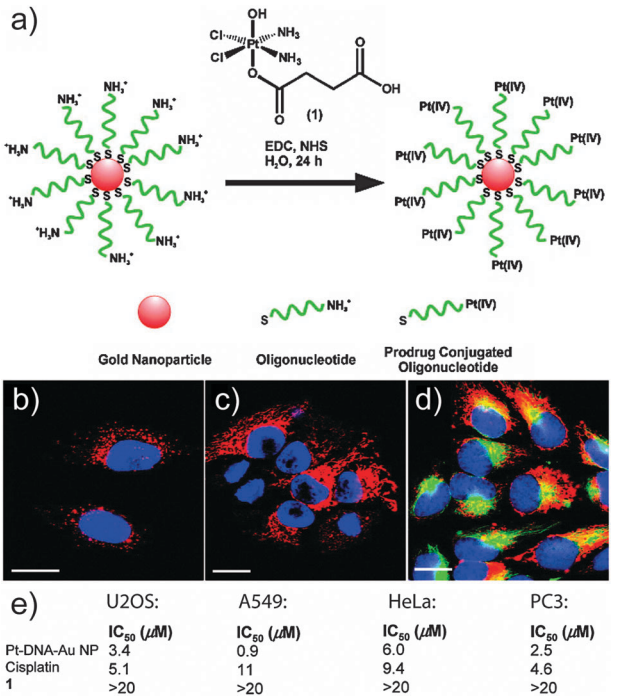


**Fig. 9** Conjugation, delivery, *in vitro* efficacy of a cisplatin prodrug-gold nanoparticle conjugate. The $Pt^{4+}$ cisplatin prodrug was conjugated (a) to amine-terminal, fluorescent, oligonucleotide-functionalized gold nanoparticles and incubated with cervical cancer cells for 6 h (b) and 12 h (c), demonstrating significant intracellular accumulation (red). Multiplexed labeling (d) of intracellular microtubules (green) and colocalization (yellow) with the nanoparticle conjugates indicated efficient delivery and endosomal escape. Half maximal inhibitory concentrations ($IC_{50}$) of Pt (e) from the nanoparticle conjugate, cisplatin, and the prodrug alone indicated significantly enhanced potency in treating bone osteosarcoma, lung adenocarcinoma, cervical carcinoma, and prostate carcinoma cells (U2SO, A549, HeLa, and PC3, respectively). Scale bars: 20 μm. Nuclei are stained blue. Reprinted with permission from ref. 48. Copyright 2010 American Chemical Society.

Strategies for the delivery of chemotherapeutic taxanes using gold nanoparticles has likewise been explored in a particularly well-characterized study by Zubarev and co-workers.[50] Using a thiol-PEGylated derivative of paclitaxel, modified at the C7 position to maintain pharmacologic activity, the group was able to conjugate 2 nm gold nanoparticles which showed excellent structural homogeneity and allowed detailed chemical analysis.

Li and co-workers have explored anthracycline conjugates of gold nanoparticles for potential photo-triggered release applications.[51] The group demonstrated high loading (63% w/w) of the DNA-intercalating mitotic inhibitor, doxorubicin (DOX), in/on 40 nm diameter PEGylated, hollow-core gold nanoparticles *via* the amine group on DOX. Loaded DOX was found to be 3.5-fold higher than that achievable using spherical particles (*i.e.* % w/w) and was effectively retained by the particles over several days in physiologic media. Both NIR photothermal heating and exposure to endosomal pH (*i.e.* 5) were found to result in significantly increased DOX release and cytotoxicity to breast cancer cells. Non-triggered conjugates also exhibited significantly lower cytotoxicity *versus* native DOX, a characteristic potentially capable of mitigating the substantial adverse side effects from DOX therapy *in vivo*.

Folate metabolism is another attractive target for anti-cancer gold nanoparticle conjugates as a number of cancer cells exhibit upregulated folate activity. Chen *et al.* have studied gold nanoparticle conjugates of methotrexate (MTX), a dihydrofolate reductase inhibitor for the treatment of primary lung tumors.[52] Here, anionic gold nanoparticles (13 nm dia) were electrostatically conjugated to the cytotoxic chemotherapeutic drug, and using various cancer cell lines, the group found that MTX potency increased 5- to 25-fold upon nanoparticle conjugation. Significantly decreased tumor mass

and volume were observed from lung tumor-bearing Black 6 mice treated with the gold nanoparticle conjugates *versus* free MTX, particles, or controls. Enhanced cytotoxicity was attributed to increased MTX influx by nanoparticle endocytosis. Anticipated prolonged accumulation/retention of the MTX-gold nanoparticle conjugates is expected to improve treatment response under *in vivo* conditions as well. Andres and co-workers have synthesized a thiol-PEGylated derivative of folate which could be easily conjugated to gold nanoparticles (10 nm dia).[53] In this case, the group showed that the folate conjugate maintained receptor binding affinity, under microscopy, exhibiting selective uptake into cells overexpressing the folate receptor and localizing about the lysosomes, endosomes, and perinuclear intracellular regions. Similar strategies involving the co-conjugation of cytotoxic drugs could be expected to exert receptor-selective anti-cancer activity.

Gold nanoparticle-targeted delivery of photosensitizer molecules for photodynamic therapy (PDT) is another strategy for the increasingly selective treatment of malignant tissues. In PDT, molecules which form singlet oxygen upon excitation are selectively delivered to malignant tissues and exposed to laser, typically NIR, radiation. Because photosensitizer molecules generally exhibit non-specific tumor accumulation and prohibitively low hydrophilicity, conjugation to PEGylated gold nanoparticle carriers is an attractive strategy with which to improve their pharmacokinetics by EPR accumulation and to lengthen their circulatory half lives. Burda and co-workers have studied the delivery of phthalocyanine photosensitizers to cervical cancer cells *in vitro* using 5 nm PEGylated gold nanoparticles.[54] Interestingly, they found that the efficiency of particle delivery and PDT was significantly higher when using labile amino linkages *versus* more strongly bonding thiols between the particle and the phthalocyanine, highlighting the importance of considering the effects of bonding interactions on subsequent treatment efficacy.

### Gold nanoparticles in gene therapy

The controlled regulation of gene expression is another method by which malignancies can be treated using gold nanotechnologies. The nuclear delivery of small interfering RNA (siRNA) is well known to selectively modulate or reduce the expression of their corresponding target genes (RNA interference, RNAi). Efficient penetration of the cell membrane and endosomal escape by siRNA, however, are major impediments to the efficient knockdown of tumor-associated genes/proteins in RNAi therapies. siRNA conjugation with nanoparticles has been shown to protect these nucleic acids from extracellular degradation, prolong circulation, facilitate cell membrane penetration, and prevent endosomal digestion in clinical settings.[55] Active and/or passive (EPR) targeting of these conjugates can also localize RNAi effects to solid tumors.

Gold nanoparticles present several opportunities for the selective delivery of siRNA and subsequent knockdown of tumorigenic proteins. Giljohann *et al.* have shown that gold colloids can be rendered RNase free by treatment with diethylpyrocarbonate and subsequent autoclaving at 121 °C (60 min).[56] Using this RNA-compatible platform, thiol-PEGylated RNA oligonucleotide strands (*i.e.* sense RNA) were conjugated to the gold particles and hybridized with complementary siRNA (antisense) sequences which were to be delivered. They showed more than two-fold greater knockdown of target protein expression in cervical cancer cells (HeLa) when the siRNA was delivered to the cells using 13 nm diameter PEGylated gold nanoparticles. Lee and co-workers have further exploited the photothermal properties of NIR absorbing gold nanorods in a similar approach, showing that externally triggered photothermal heating of the nanoparticle–siRNA conjugate above the melting temperature of the duplex sequences facilitated their controlled intracellular delivery and knockdown of oncogenic proteins.[57] They conjugated a thiolated sense RNA sequence to gold nanorods and hybridized antisense RNA which targets HER2 oncogenic protein, commonly upregulated in breast cancers. siRNA release was demonstrated in a laser wavelength- and power-dependent manner, with no significant cytotoxicity. Corresponding *ca.* 10% knockdown of HER2 protein was demonstrated in breast carcinoma cells (BT474) following treatment and laser exposure of the siRNA gold nanorods, but not from controls, laser, or sham siRNA.

Lu *et al.* have combined the above NIR photothermal and RNAi strategies with active particle targeting to achieve selective siRNA delivery and chemosensitization of cervical cancer *in vivo*.[18] The group conjugated hollow gold nanospheres with thiol-PEGylated folic acid for selective folate receptor targeting and a thiolated sense RNA strand complemented by an siRNA sequence for *NF-κB* to allow chemosensitization to irinotecan therapy. *NF-κB* is a transcription factor which regulates a number of genes associated with malignant growth/progression. The chemotherapeutic irinotecan is a topoisomerase 1 inhibitor and analog of camptothecin which inhibits DNA replication/transcription and is primarily applied in colon cancer treatment. Using this gold nanoconjugate, the authors demonstrated photothermal triggered release and endosomal escape of siRNA *in vitro*. They also showed greater than 4-fold increased tumor uptake from folate *versus* untargeted nanoparticles and *ca.* 4-fold down-regulation of *NF-κB* in tumors exposed to NIR radiation relative to those un-exposed in the same mouse. Photothermal transfection and combined chemotherapy showed significantly greater apoptotic destruction *versus* untargeted, sham siRNA, and un-exposed tumors. This study particularly highlights the tremendous versatility and multifunctionality of anti-cancer gold nanoparticle conjugates in targeted therapeutic treatment strategies for cancer.

### Gold nanoparticles as intrinsic antineoplastic agents

Although many oncologic applications of gold nanoparticles rely on extrinsic functionalization/activation, gold nanostructures can also exhibit intrinsic antineoplastic properties. Like chemo- and radio-therapy, the selective regulation of cell growth and division by gold nanoparticles can serve as another potent anti-cancer treatment strategy. Many reports have shown that targeted gold nanoparticles are capable of altering the cell cycle, including cell division, signaling, and proliferation. Because malignant cells are increasingly

sensitive to cell cycle disruption and also less capable of repairing such damages, gold nanoparticles can be used as cancer-selective cytotoxic agents.

As discussed previously, the extent of tumor growth and malignant progression is highly dependent on the formation of new blood vessels, angiogenesis, a process primarily mediated by signaling associated with vascular permeability factor/vascular endothelial growth factor 165 (VPF/VEGF-165). Selective inhibition of VPF/VEGF-165 activity is one method by which angiogenic growth can be mitigated in anti-cancer treatments. Mukhopadhyay and co-workers have recently studied the effects of spherical gold nanoparticles on VEGF-165-dependent proliferation in human umbilical vascular endothelial cells (HUVEC).[58] Their results showed that these gold particles significantly inhibited VEGF-165-induced cell proliferation of HUVEC cells (5 nm dia, citrate-capped, 335–670 nM, 24 h). Using X-ray photoelectron spectroscopy (XPS), they found that the gold nanoparticles bound directly to the heparin-binding domain of VEGF-165 through sulfur and/or nitrogen bonds, an interaction which significantly inhibits VEGF-165's ability to associate with cell surface receptors necessary for angiogenic signaling and proliferation. Further, they showed that gold nanoparticles had no effect on signaling/proliferation associated with a non-heparin binding growth factor, VEGF-121. The group later explored the ability of gold nanoparticles to inhibit VEGF-165-induced angiogenesis and vascular permeability *in vivo,* observing a significant reduction of angiogenic activity in ovarian tumor-bearing nude mice when the gold nanoparticles were intradermally administered (2 × 10 μL of 670 nM).[59] A significant decrease in vascular permeability was also observed following injection of the gold nanoparticle mixture, combined effects which could be potentially applied in future anti-cancer treatments. Because surface stabilization of the particles is required for systemic administration, this method would most likely be applied *via* interstitial or transdermal injection into solid tumors.

Selective modulation of the cell cycle is another strategy by which gold nanoparticles can be applied in anti-cancer therapies. Xing and co-workers have explored changes in the cell cycle and sensitization to radiotherapy in a radiation-resistant human prostate carcinoma cells line (DU-145) treated with glucose-capped gold nanoparticles (10.8 nm dia) *in vitro*.[60] The glucose–gold nanoparticle conjugates were shown to arrest the prostate cancer cells in the G2/M phase of the cell cycle, the phase in which cells are most sensitive to radiation damage (15 nM, 2 h). Accumulation of the cells in G2/M was shown to result from upregulated expression of cyclin E protein, a promoter of the so-called cell cycle "checkpoint kinase", which regulates transition from G1 to S and accelerates progression through G1 (1.2-fold, 24 h; 1.5-fold, 48 h). Radiosensitization of prostate cancer cells treated with glucose-gold nanoparticle conjugates is expected to increase the efficacy of subsequent radiotherapy treatments and to minimize adverse side-effects by lowering threshold exposure levels.

Because cancer cells are increasingly sensitive to cell cycle disruption and DNA damage, gold nanoparticles which induce such effects can be selectively delivered to malignant cells or administered at dosages below that necessary to damage normal tissues to achieve oncologic effect. Our lab has recently shown that gold nanoparticles targeted to cell nuclei selectively induce DNA damage, cytokinesis arrest, and programmed cell death (*i.e.* apoptosis) in malignant cells (Fig. 10).[17] Kang *et al.* conjugated PEGylated gold nanospheres (30 nm dia) with a thiolated, linear RGD peptide (*i.e.* arginine–glycine–aspartic acid) known to target alpha V beta integrins overexpressed on the surfaces of cancer cells. An NLS (nuclear localization sequence) peptide known to associate with cytoplasmic importins which translocate to the nuclear pore complex was also co-conjugated to the RGD particles. Time-resolved dark-field scattering microscopy of live squamous cell carcinoma cells (HSC-3) treated with the RGD/NLS gold nanoparticles showed apparent cytokinesis arrest (0.4 nM, 24 h) while non-malignant keratinocyte (HaCaT) cells continued to divide normally. Treatment with

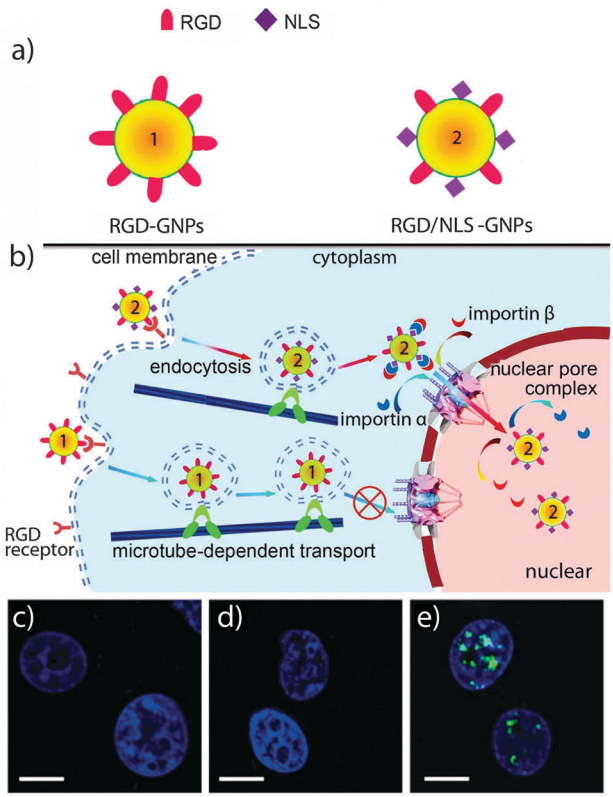


**Fig. 10** Schematic illustrating selective DNA damage of malignant cells using peptide-targeted gold nanoparticle conjugates. PEGylated gold nanoparticles (30 nm dia) were conjugated (a) with a thiolated-RGD peptide (1) and further co-conjugated with a nuclear localization sequence (NLS) peptide (2). RGD conjugation facilitated particle endocytosis and cytoplasmic delivery (b) by association with alpha V beta integrins overexpressed on the surfaces of cancer cells. NLS-mediated perinuclear localization of the particles was achieved by association with cytoplasmic importins which translocate to the nuclear pore complex. Immuno-fluorescence microscopy of control (c) and RGD nanoconjugate-treated (d) carcinoma cell nuclei (blue) showed no indication of DNA damage while RGD/NLS nanoconjugate-treated carcinoma cells (e) showed substantial DNA double strand breaks (green). Reprinted with permission from ref. 17. Copyright 2010 American Chemical Society.

RGD conjugates showed no such behavior in either cell line. Immuno-fluorescence microscopy of malignant cells treated with the RGD/NLS conjugates indicated significant DNA double strand breaks, while non-cancerous cells displayed no damage. RGD-targeted conjugates also showed no such breaks with either cell line. Flow cytometry indicated selective damage to malignant cells treated with the RGD/NLS particles, showing *ca.* 20% greater apoptosis than non-malignant cells. The selective, anti-proliferative properties of these targeted nanoparticle conjugates could, in the future, serve in anti-cancer treatments functionally analogous to current radiotherapy and chemotherapy methods.

## Conclusions

Gold nanoparticles present tremendous opportunities for the design of next-generation, multimodal anti-cancer treatment strategies involving photothermal therapy, drug delivery, gene therapy, and cell cycle regulation. Due to their multivalency and functional versatility, these particle conjugates can exhibit increased targeting selectivity, augmented binding affinity, long circulatory half life, high biocompatibility, rapid transport kinetics, and size-enhanced tumor uptake. The optical and electronic properties of gold nanoparticles can further provide high contrast in photothermal therapeutic treatments, as well as photoacoustic, optical coherence, and X-ray CT imaging. The intrinsic biomolecular interactions of gold nanoparticles can additionally provide cancer-selective cytotoxic activity. Together, these properties comprise a highly multifunctional platform on which increasingly selective and potent oncologic treatment methods can be designed now and in the future.

## Acknowledgements

MAE and co-workers acknowledge generous support from the U.S. National Institute of Health (1U01CA151802-01) and the Center for Nanostructured Materials Technology under the 21st Century Frontier R&D Programs of the Korean Ministry of Education, Science, and Technology (Grant No. 08K1501-01910). ECD thanks support from Mark Prautznitz and The Center for Drug Design, Development, and Delivery (CD4) Predoctoral Fellowship, as well as Arturo Belano and D. F. Wallace for helpful discussions. BK thanks support from the China Scholar Council (2008683010).

## References

1 X. H. Huang, P. K. Jain, I. H. El-Sayed and M. A. El-Sayed, *Nanomedicine*, 2007, **2**, 681–693.
2 P. Ghosh, G. Han, M. De, C. K. Kim and V. M. Rotello, *Adv. Drug Delivery Rev.*, 2008, **60**, 1307–1315.
3 S. Lal, S. E. Clare and N. J. Halas, *Acc. Chem. Res.*, 2008, **41**, 1842–1851.
4 D. A. Giljohann, D. S. Seferos, W. L. Daniel, M. D. Massich, P. C. Patel and C. A. Mirkin, *Angew. Chem., Int. Ed.*, 2010, **49**, 3280–3294.
5 M. Faraday, *Philos. Trans. R. Soc. London*, 1857, **147**, 145–181.
6 J. Turkevich, P. C. Stevenson and J. Hillier, *Discuss. Faraday Soc.*, 1951, **11**, 55–75.
7 G. Frens, *Nature*, 1973, **241**, 20–22.
8 X. Huang, S. Neretina and M. A. El-Sayed, *Adv. Mater.*, 2009, **21**, 4880–4910.
9 S. J. Oldenburg, R. D. Averitt, S. L. Westcott and N. J. Halas, *Chem. Phys. Lett.*, 1998, **288**, 243–247.
10 J. Chen, J. M. McLellan, A. Siekkinen, Y. Xiong, Z.-Y. Li and Y. Xia, *J. Am. Chem. Soc.*, 2006, **128**, 14776–14777.
11 S. E. Skrabalak, J. Chen, Y. Sun, X. Lu, L. Au, C. M. Cobley and Y. Xia, *Acc. Chem. Res.*, 2008, **41**, 1587–1595.
12 J. C. Love, L. A. Estroff, J. K. Kriebel, R. G. Nuzzo and G. M. Whitesides, *Chem. Rev.*, 2005, **105**, 1103–1170.
13 A. J. Bard and L. R. Faulkner, *Electrochemical Methods: Fundamentals and Applications*, John Wiley & Sons, Inc., New York, 2nd edn, 2001.
14 C. Tassa, J. L. Duffner, T. A. Lewis, R. Weissleder, S. L. Schreiber, A. N. Koehler and S. Y. Shaw, *Bioconjugate Chem.*, 2009, **21**, 14–19.
15 G. von Maltzahn, J.-H. Park, A. Agrawal, N. K. Bandaru, S. K. Das, M. J. Sailor and S. N. Bhatia, *Cancer Res.*, 2009, **69**, 3892–3900.
16 E. C. Dreaden, S. C. Mwakwari, Q. H. Sodji, A. K. Oyelere and M. A. El-Sayed, *Bioconjugate Chem.*, 2009, **20**, 2247–2253.
17 B. Kang, M. A. Mackey and M. A. El-Sayed, *J. Am. Chem. Soc.*, 2010, **132**, 1517–1519.
18 W. Lu, G. Zhang, R. Zhang, L. G. Flores, Q. Huang, J. G. Gelovani and C. Li, *Cancer Res.*, 2010, **70**, 3177–3188.
19 S. Link and M. A. El-Sayed, *Int. Rev. Phys. Chem.*, 2000, **19**, 409–453.
20 E. I. Galanzha, E. V. Shashkov, T. Kelly, J.-W. Kim, L. Yang and V. P. Zharov, *Nat. Nanotechnol.*, 2009, **4**, 855–860.
21 A. K. Iyer, G. Khaled, J. Fang and H. Maeda, *Drug Discovery Today*, 2006, **11**, 812–818.
22 W. Lu, C. Xiong, G. Zhang, Q. Huang, R. Zhang, J. Z. Zhang and C. Li, *Clin. Cancer Res.*, 2009, **15**, 876–886.
23 C. H. J. Choi, C. A. Alabi, P. Webster and M. E. Davis, *Proc. Natl. Acad. Sci. U. S. A.*, 2010, **107**, 1235–1240.
24 M. P. Melancon, W. Lu, Z. Yang, R. Zhang, Z. Cheng, A. M. Elliot, J. Stafford, T. Olson, J. Z. Zhang and C. Li, *Mol. Cancer Ther.*, 2008, **7**, 1730.
25 B. D. Chithrani, A. A. Ghazani and W. C. W. Chan, *Nano Lett.*, 2006, **6**, 662–668.
26 W. Jiang, Y. S. KimBetty, J. T. Rutka and C. W. Chan, *Nat. Nanotechnol.*, 2008, **3**, 145–150.
27 M. Longmire, P. L. Choyke and H. Kobayashi, *Nanomedicine*, 2008, **3**, 703–717.
28 D. E. Owens III and N. A. Peppas, *Int. J. Pharm.*, 2006, **307**, 93–102.
29 R. S. Obach, F. Lombardo and N. J. Waters, *Drug Metab. Dispos.*, 2008, **36**, 1385–1405.
30 W.-S. Cho, M. Cho, J. Jeong, M. Choi, B. S. Han, H.-S. Shin, J. Hong, B. H. Chung, J. Jeong and M.-H. Cho, *Toxicol. Appl. Pharmacol.*, 2010, **245**, 116–123.
31 H. Bert, W. Peter, A. Olaf, D. Annette, S. Geetha, K. Thoralf, F. Roland and R. Hanno, *Crit. Rev. Oncol. Hemat.*, 2002, **43**, 33–56.
32 E. B. Dickerson, E. C. Dreaden, X. Huang, I. H. El-Sayed, H. Chu, S. Pushpanketh, J. F. McDonald and M. A. El-Sayed, *Cancer Lett.*, 2008, **269**, 57–66.
33 D. S. Coffey, R. H. Getzenberg and T. L. DeWeese, *J. Am. Med. Assoc.*, 2006, **296**, 445–448.
34 R. Weissleder, *Nat. Biotechnol.*, 2001, **19**, 316–317.
35 C. M. Pitsillides, E. K. Joe, X. Wei, R. R. Anderson and C. P. Lin, *Biophys. J.*, 2003, **84**, 4023–4032.
36 I. H. El-Sayed, X. Huang and M. A. El-Sayed, *Cancer Lett.*, 2006, **239**, 129–135.
37 L. R. Hirsch, R. J. Stafford, J. A. Bankson, S. R. Sershen, B. Rivera, R. E. Price, J. D. Hazle, N. J. Halas and J. L. West, *Proc. Natl. Acad. Sci. U. S. A.*, 2003, **100**, 13549–13554.
38 D. P. O'Neal, L. R. Hirsch, N. J. Halas, J. D. Payne and J. L. West, *Cancer Lett.*, 2004, **209**, 171–176.
39 X. Huang, I. H. El-Sayed and M. A. El-Sayed, *J. Am. Chem. Soc.*, 2006, **128**, 2115–2120.
40 J. Chen, D. Wang, J. Xi, L. Au, A. Siekkinen, A. Warsen, Z. Y. Li, H. Zhang, Y. Xia and X. Li, *Nano Lett.*, 2007, **7**, 1318.
41 C. Kim, E. C. Cho, J. Chen, K. H. Song, L. Au, C. Favazza, Q. Zhang, C. M. Cobley, F. Gao, Y. Xia and L. V. Wang, *ACS Nano*, 2010, **4**, 4559–4564.

42 M. Hu, J. Chen, Z.-Y. Li, L. Au, G. V. Hartland, X. Li, M. Marquez and Y. Xia, *Chem. Soc. Rev.*, 2006, **35**, 1084–1094.
43 J. R. Cole, N. A. Mirin, M. W. Knight, G. P. Goodrich and N. J. Halas, *J. Phys. Chem. C*, 2009, **113**, 12090–12094.
44 P. Cherukuri, E. S. Glazer and S. A. Curley, *Adv. Drug Delivery Rev.*, 2010, **62**, 339–345.
45 J. Cardinal, J. R. Klune, E. Chory, G. Jeyabalan, J. S. Kanzius, M. Nalesnik and D. A. Geller, *Surgery*, 2008, **144**, 125–132.
46 J. F. Hainfeld, F. A. Dilmanian, Z. Zhong, D. N. Slatkin, J. A. Kalef-Ezra and H. M. Smilowitz, *Phys. Med. Biol.*, 2010, **55**, 3045.
47 G. F. Paciotti, D. G. Kingston and L. Tamarkin, *Drug Dev. Res.*, 2006, **67**, 47–54.
48 S. Dhar, W. L. Daniel, D. A. Giljohann, C. A. Mirkin and S. J. Lippard, *J. Am. Chem. Soc.*, 2009, **131**, 14652–14653.
49 S. D. Brown, P. Nativo, J.-A. Smith, D. Stirling, P. R. Edwards, B. Venugopal, D. J. Flint, J. A. Plumb, D. Graham and N. J. Wheate, *J. Am. Chem. Soc.*, 2010, **132**, 4678–4684.
50 J. D. Gibson, B. P. Khanal and E. R. Zubarev, *J. Am. Chem. Soc.*, 2007, **129**, 11653–11661.
51 J. You, G. Zhang and C. Li, *ACS Nano*, 2010, **4**, 1033–1041.
52 Y. H. Chen, C. Y. Tsai, P. Y. Huang, M. Y. Chang, P. C. Cheng, C. H. Chou, D. H. Chen, C. R. Wang, A. L. Shiau and C. L. Wu, *Mol. Pharmaceutics*, 2007, **4**, 713–722.
53 V. Dixit, J. Van den Bossche, D. M. Sherman, D. H. Thompson and R. P. Andres, *Bioconjugate Chem.*, 2006, **17**, 603–609.
54 Y. Cheng, A. C. Samia, J. Li, M. E. Kenney, A. Resnick and C. Burda, *Langmuir*, 2009, **26**, 2248–2255.
55 M. E. Davis, J. E. Zuckerman, C. H. J. Choi, D. Seligson, A. Tolcher, C. A. Alabi, Y. Yen, J. D. Heidel and A. Ribas, *Nature*, 2010, **464**, 1067–1070.
56 D. A. Giljohann, D. S. Seferos, A. E. Prigodich, P. C. Patel and C. A. Mirkin, *J. Am. Chem. Soc.*, 2009, **131**, 2072–2073.
57 S. E. Lee, G. L. Liu, F. Kim and L. P. Lee, *Nano Lett.*, 2009, **9**, 562–570.
58 R. Bhattacharya, P. Mukherjee, Z. Xiong, A. Atala, S. Soker and D. Mukhopadhyay, *Nano Lett.*, 2004, **4**, 2479–2481.
59 P. Mukherjee, R. Bhattacharya, P. Wang, L. Wang, S. Basu, J. A. Nagy, A. Atala, D. Mukhopadhyay and S. Soker, *Clin. Cancer Res.*, 2005, **11**, 3530–3534.
60 W. Roa, X. J. Zhang, L. H. Guo, A. Shaw, X. Y. Hu, Y. P. Xiong, S. Gulavita, S. Patel, X. J. Sun, J. Chen, R. Moore and J. Z. Xing, *Nanotechnology*, 2009, **20**, 375101.

 